RSC Advances

PAPER

View Article Online
View Journal | View Issue

Cite this: *RSC Adv.*, 2023, **13**, 22079

Enzyme and pH dual responsive linear-dendritic block copolymer micelles based on a phenylalanyl–lysine motif and peripherally ketal-functionalized dendron as potential drug carriers†

Yujia Wang,‡ Wenjie Song,‡ Lijun Bao, Junwu Wei, Yangyang Qian and Yunmei Bi *

Stimuli–responsive linear-dendritic block copolymers (LDBCs) have attracted significant research attention as novel drug carriers. We report here three generations of new enzyme and pH dual responsive linear-dendritic block copolymers (LDBCs) with a phenylalanyl–lysine (Phe–Lys) dipeptide linking hydrophilic linear poly(*N*-vinylpyrrolidone) (PNVP) and a hydrophobic peripherally ketal-functionalized dendron derived from 2,2′-bis(hydroxymethyl)propionic acid (bis-MPA). The LDBCs are synthesized *via* a combination of interchange of xanthates/reversible addition–fragmentation chain transfer (MADIX/RAFT) polymerization of *N*-vinylpyrrolidone (NVP) and "chain-first" strategy. Their structures are confirmed by ^{1}H NMR spectra. The gel permeation chromatograph (GPC) analysis revealed that the LDBCs have a narrow molecular weight distribution (PDI ≤ 1.25). The amphiphilic LDBCs can self-assemble into spherical nanomicelles in aqueous solution. The presence of enzyme or/and the change of pH cause disassembly of micelles to release encapsulated cargos. The release rates of the guest molecules are faster in buffer solution at pH 5.0 than those upon the addition of the activating enzyme and can be fine-tuned by changing the generation of bis-MPA dendrons. The combination of enzyme and pH dual stimuli results in significantly accelerated and more complete release of the loaded hydrophobic guests. The cell viability assay confirmed the favorable biocompatibility until the LDBC micelle concentration reached 800 μg mL^{-1}. These results indicate that the LDBCs can be considered as a good candidate for targeting drug delivery.

Received 6th June 2023
Accepted 12th July 2023

DOI: 10.1039/d3ra03790h

rsc.li/rsc-advances

Introduction

Stimuli–responsive linear-dendritic block copolymers (LDBCs) have drawn increasing research interest in recent years because of combining the ability to respond to various stimuli (such as light, temperature, pH and enzymes) and different polymeric architectures for a broad range of applications, including drug delivery, gene therapy and materials science.[1–8] In this regard, enzyme responsive LDBCs are especially intriguing owing to high selectivity and favorable efficiency of enzyme-catalyzed reactions.[9] Moreover, since some enzymes are overexpressed in diseased states, by incorporating enzyme labile linkages, polymeric nanoparticles can be constructed to release the loaded drug at desired sites, and are excellent candidates for drug targeted delivery.[10–12] Amir's group has reported a series of LDBCs based on a linear hydrophilic polyethyleneglycol (PEG) and a dendron with enzyme-cleavable hydrophobic end groups.[9,13–15] Our group obtained some LDBCs composed of a hydrophilic linear enzyme responsive poly(hydroxyethyl L-glutamine) (PHEG) and a hydrophobic dendron derived from cysteamine or 2,2′-bis(hydroxymethyl)propionic acid (bis-MPA).[16] Some LDBCs based on linear poly(*N*-vinylpyrrolidone) (PNVP) and enzyme responsive dendritic phenylalanyl–lysine (Phe–Lys) dipeptides have also been synthesized.[17] The enzyme responsive moieties of these LDBCs have been incorporated into their linear chain, dendritic blocks and periphery of dendrons. However, to date, there has been no any report on an enzyme–responsive motif is introduced at the junction point between the hydrophilic linear chain and hydrophobic dendritic block of amphiphilic LDBCs.

In the past decade, pH–responsive LDBCs have been developed for the application of targeted and controlled drug delivery since the numerous pH gradients exist in both normal and pathophysiological states.[18] Many pH–responsive units such as carboxylic acid,[19,20] amino-ester,[21] amino acid,[22] amines,[23] acetal groups[5,24] and hydrazone bonds[25] have been incorporated into LDBCs. The pH–responsive polymers with highly sensitive ketal linkages have generated significant interest as promising

College of Chemistry and Chemical Engineering, Yunnan Normal University, Kunming 650500, China. E-mail: yunmeibi@hotmail.com

† Electronic supplementary information (ESI) available. See DOI: https://doi.org/10.1039/d3ra03790h

‡ These authors contributed equally to this work.

candidates for tumor-targeted drug delivery. This is attributed to their distinctive features that ketal linkages hydrolyze into neutral alcohols and ketones could avoiding inflammatory problems compared with the acidic degradation products of polyesters and polyorthoesters.[26] Moreover, ketal linkages were more sensitive to the lower pH environment of tumors or phagosomes than hydrazones but were more stable than these linkages in the pH 7.4 of the blood.[27] However, to the best of our knowledge, the pH–responsive LDBCs with ketal peripheries have so far not been reported.

Although many single stimulus responsive LDBCs have been obtained, dual responsive LDBCs have been relatively underexplored, especially systems that exhibit enzyme responsive behavior.[24,28,29] There are large variations in physiological conditions between normal microenvironments and diseased sites, thus single responsive polymer materials could not achieve the desired goals in a complex physiological microenvironment. The integration of several responsive moieties within one polymer is highly desired for biomedical applications.[30–32] In particular, the combination of enzyme and pH stimuli is appropriate to design polymer nanocarriers for tumour targeted delivery of drugs since lower pH values in tumours relative to normal tissues.[33–35] Additionally, it is well known that some enzymes (such as matrix metallo proteinases,[36] cathepsin B,[37] alkaline phosphatase,[38] trypsin[39]) are overexpressed in tumor cells due to the needs of proliferation.

In this study, an enzyme cleavable phenylalanyl–lysine (Phe–Lys) dipeptide is used as a linkage between hydrophilic linear poly(*N*-vinylpyrrolidone) (PNVP) and a hydrophobic peripherally ketal-functionalized dendron derived from 2,2′-dimethylolpropionic acid (bis-MPA) to obtain enzyme and pH dual responsive LDBCs. Their self-assembly behavior in aqueous solution and the release kinetics of the encapsulated guest molecules in response to enzyme or pH stimulus and combination of dual stimuli have been investigated. The cytotoxicity of the LDBCs was tested in human lung epithelial cells (BEAS-2B) and human liver cancer cells (SMMC-7721). The LDBCs could self-assemble into spherical nanomicelles and disassembly to release loaded drug in various microenvironment which typically exist in cancer cells (Scheme 1).

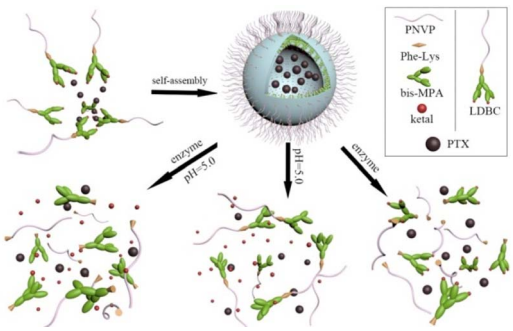

Scheme 1 Illustration of self-assembly and disassembly of the LDBCs to release encapsulated cargos in presence of enzyme or/and the change of pH.

Experimental

Materials

α,α-Azobisisobutyronitrile (AIBN) (98%, Aldrich) was recrystallized twice from methanol. *N*-Vinylpyrrolidone (NVP) (98%, Sinopharm Chemical Reagent) was distilled under reduced pressure and then stored at 4 °C. Isopropylidene-2,2-bis(oxymethyl)propionic anhydride was prepared according to literature method.[40,41]

Characterization

^{1}H NMR spectra were obtained on a Bruker DRX-500 spectrometer in $CDCl_3$ or D_2O. GPC analyses were performed on a Waters 2690D separations module and a Waters 2414 refractive index detector (RI) with Styragel HR3 and HR4 columns (Waters) using DMF as eluent at 40 °C at a flow rate of 0.3 mL min^{-1}. The system was calibrated with poly(methyl methacrylate) standards. Transmission electron microscopy (TEM) images were obtained using a JEM-2100 transmission electron microscope operating at an accelerating voltage of 200 kV. Size and distribution of the nanoparticles were characterized by ZetaPALS particle sizing systems (Brookhaven instruments).

Synthesis of PNVP-Phe-NH_2

PNVP-Phe-NH_2 was synthesized according to the method reported in our previous work.[15] ^{1}H NMR in $CDCl_3$, δ (ppm): 1.19–1.28 (m, CH_3), 1.52–1.89 (m, CH_2), 1.89–2.15 (m, CH_2), 2.15–2.96 (m, O=CCH_2), 2.99–3.48 (m, NCH_2), 3.48–4.08 (m, NCH), 7.01–7.53 (m, C_6H_5).

Synthesis of PNVP-Phe-Lys-NHBoc

To a solution of (Fmoc)lys(Boc)-OH (0.18 g, 0.30 mmol) in 10 mL of DMF was added PNVP-Phe-NH_2 (1.2 g, 0.1 mmol) and 1-hydroxybenzotriazole (HOBt) (13.51 mg, 0.1 mmol). After stirring for 30 min, *N*,*N*-diisopropylcarbodiimide (DIC) (0.06 mL, 0.4 mmol) was added. The reaction mixture was stirred at room temperature for 24 h. The crude product were precipitated and washed by cold ether. The precipitate was dissolved in distilled water, dialyzed for 3 days, and lyophilized to give a white solid. The yield was 97.5%. ^{1}H NMR in $CDCl_3$, δ (ppm): 1.18–1.29 (m, CH_3), 1.51–1.89 (m, CH_2), 1.89–2.15 (m, CH_2), 2.15–2.95 (m, O=CCH_2), 2.95–3.47 (m, NCH_2), 3.47–4.10 (m, NCH), 7.02–7.54 (m, Ar–H).

Synthesis of PNVP-Phe-Lys-NH_2

To a solution of PNVP-Phe-Lys-NHBoc (0.1 mmol) in 4 mL of DMF was added trifluoroacetic acid to adjust the pH value of the solution to 4–5. After stirring for 6 h, the reaction mixture was neutralized with NaOH solution. After filtration and evaporation of the solvent, the residue was dissolved in water, dialyzed for 3 days, and then lyophilized to obtain a white solid product in a yield of 84.4%. ^{1}H NMR in $CDCl_3$, δ (ppm): 1.18–1.29 (m, CH_3), 1.52–1.89 (m, CH_2), 1.89–2.14 (m, CH_2), 2.14–2.95 (m, O=CCH_2), 2.95–3.48 (m, NCH_2), 3.48–4.09 (m, NCH), 7.02–7.53 (m, Ar–H).

Synthesis of PNVP-Phe-Lys-*b*-G_1

PNVP-Phe-Lys-NH_2 (1.25 g, 0.1 mmol), isopropylidene-2,2-bis(oxymethyl)propionic anhydride (49.6 mg, 0.15 mmol) and DMAP (2.4 mg, 0.02 mmol) were dissolved in 20 mL of DMF/NEt_3 solution (v/v = 3/1). After stirring for 40 h at room temperature, the reaction mixture was precipitated three times by cold ether. The precipitate was collected and dissolved in distilled water, dialyzed for 3 days, and then lyophilized to obtain a white solid product in a yield of 92.3%. ^{1}H NMR in $CDCl_3$, δ (ppm): 1.19–1.29 (m, CH_3), 1.42 (s, CH_3), 1.50–1.88 (m, CH_2), 1.88–2.14 (m, CH_2), 2.14–2.63 (m, O=CCH_2), 2.91–3.48 (m, NCH_2), 3.48–4.09 (m, NCH), 7.01–7.52 (m, Ar–H).

Synthesis of PNVP-Phe-Lys-*b*-G_1-OH

1.27 g (0.1 mmol) of PNVP-Phe-Lys-*b*-G_1 was dissolved in 50 mL of THF/methanol solution (v/v = 4/3). H_2SO_4 was added to adjust the pH value of the solution to 3. After stirring for 20 h at room temperature, the reaction mixture was neutralized with $NH_3 \cdot H_2O$ and filtered to remove ammonium sulfate. The solvent was distilled off and the residue was added to distilled water, dialyzed for 3 days, and then lyophilized to obtain a white solid in a yield of 80.1%. ^{1}H NMR in $CDCl_3$, δ (ppm): 1.20–1.30(m, CH_3), 1.50–1.89 (m, CH_2), 1.89–2.14 (m, CH_2), 2.14–2.65 (m, O=CCH_2), 2.92–3.47 (m, NCH_2), 3.48–4.08 (m, NCH), 4.24–4.39 (m, OCH_2), 7.02–7.50 (m, Ar–H).

Synthesis of PNVP-Phe-Lys-*b*-G_2

PNVP-Phe-Lys-*b*-G_1-OH (1.27 g, 0.1 mmol), isopropylidene-2,2-bis(oxymethyl)propionic anhydride (0.40 g, 1.2 mmol) and (0.15 g, 1.2 mmol) of DMAP were dissolved in 5 mL of pyridine/CH_2Cl_2 solution (v/v = 3/2). After stirring for 48 h at room temperature, the reaction mixture was precipitated three times by cold ether. The precipitate was collected and dissolved in water, dialyzed for 3 days, and then lyophilized to obtain a white solid product in a yield of 89.2%. ^{1}H NMR in $CDCl_3$, δ (ppm): 1.19–1.30 (m, CH_3), 1.42 (s, CH_3), 1.52–1.89 (m, CH_2), 1.89–2.14 (m, CH_2), 2.14–2.62 (m, O=CCH_2), 2.94–3.48 (m, NCH_2), 3.48–4.09 (m, NCH), 4.22–4.38 (m, OCH_2), 7.02–7.52 (m, Ar–H).

Synthesis of PNVP-Phe-Lys-*b*-G_2-OH

PNVP-Phe-Lys-*b*-G_2-OH was synthesized by the same general procedure described for the synthesis of PNVP-Phe-Lys-*b*-G_1-OH. From PNVP-Phe-Lys-*b*-G_2 (1.27 g, 0.1 mmol), THF (32 mL), methanol (24 mL) and H_2SO_4 were obtained as a white solid in a yield of 76.0% (0.99 g). ^{1}H NMR in $CDCl_3$, δ (ppm): 1.21–1.31 (m, CH_3), 1.51–1.89 (m, CH_2), 1.89–2.14 (m, CH_2), 2.14–2.62 (m, O=CCH_2), 2.96–3.48 (m, NCH_2), 3.49–4.09 (m, NCH), 4.24–4.41 (m, OCH_2), 7.02–7.52 (m, Ar–H).

Preparation of PNVP-Phe-Lys-*b*-G_3

PNVP-Phe-Lys-*b*-G_3 was synthesized by the same general procedure described for the synthesis of PNVP-Phe-Lys-*b*-G_2. From DMAP (0.29 g, 2.4 mmol), pyridine (3 mL), CH_2Cl_2 (3 mL), PNVP-Phe-Lys-*b*-G_2-OH (1.29 g, 0.1 mmol) and isopropylidene-2,2-bis(oxymethyl)propionic anhydride (0.79 g, 2.4 mmol) were obtained as a white solid in a yield of 97.0% (1.25 g). ^{1}H NMR in $CDCl_3$, δ(ppm): 1.21–1.30 (m, CH_3), 1.43 (s, CH_3), 1.51–1.88 (m, CH_2), 1.88–2.14 (m, CH_2), 2.14–2.63 (m, O=CCH_2), 2.95–3.47 (m, NCH_2), 3.49–4.09 (m, NCH), 4.59–4.88 (m, OCH_2),7.02–7.54 (m, Ar–H).

Critical micelle concentration (CMC)

The CMC was determined using pyrene as a fluorescence probe according to a procedure as described previously.[42]

Encapsulation of drug or dye in polymer micelles

PNVP-Phe-Lys-*b*-G_n (n = 1–3) (10 mg) and Nile red were dissolved in acetone. PBS buffer was added dropwise to the solution under vigorous stirring. Then acetone was thoroughly removed by evaporation at room temperature. The precipitate of un-encapsulated Nile red was removed by centrifugation at 3000 rpm for 10 min. Fluorescence spectra of Nile red were recorded on a luminescence spectrometer. The emission spectra were recorded ranging from 570 to 800 nm with an excitation wavelength of 550 nm.

PNVP-Phe-Lys-*b*-G_3 and PTX were dissolved in ethanol, then deionized water was added slowly after complete dissolution. Ethanol was removed and the residual solution was centrifuged at high speed for 30 minutes. The drug-loaded micelles were prepared by freeze-drying the supernatant. The freeze-dried drug-loaded micelles were diluted with ethanol, their UV absorbance was determined at 227 nm, and the content of PTX in the drug-loaded micelles was calculated. The entrapping efficiency and drug-loading capacity were calculated according to the following formulas:

$$\text{entrapping efficiency} = \frac{\text{amount of drug in micelles}}{\text{initial amount of drug}} \times 100\%$$

$$\text{drug-loading capacity} = \frac{\text{amount of drug in micelles}}{\text{initial amount of micelles}} \times 100\%$$

Transmission electron microscopy (TEM)

A drop of micellar solution (1 mg mL^{-1}, or Nile red-loaded micelles, or dealt with trypsin) was placed on a copper grid coated with a carbon film and dried before TEM measurement.

In vitro release of PTX from PNVP-Phe-Lys-*b*-G_3 micelles

Trypsin solution was added to 15 mL drug-loaded micelle solution (1.0 mg mL^{-1}) or PTX solution, and the final trypsin concentration was 0, 25 and 75 μM, respectively. The solution was placed into pre-swelled dialysis bag (3 kDa) that was immersed into 150 mL PBS solution (pH 7.4, containing 0.5% Tween 80) or acetate buffer solution (pH 5.0, containing 0.5% Tween 80) at 37 °C. At regular intervals of time, 2 mL of aliquots of the solutions were taken out and the amount of released PTX was determined by UV analysis.

Cytotoxicity tests

In vitro cytotoxicity of PNVP-Phe-Lys-*b*-G_2 and PNVP-Phe-Lys-*b*-G_3 micelles against human lung epithelial cells (BEAS-2B) and human liver cancer cells (SMMC-7721) were determined by MTS assay as described previously.[17]

Results and discussion

Synthesis and characterization of PNVP-Phe-Lys-*b*-G_n

Three generations of new enzyme and pH responsive LDBCs with a phenylalanyl–lysine (Phe–Lys) dipeptide linking hydrophilic linear poly(*N*-vinylpyrrolidone) (PNVP) block and a hydrophobic acid-labile acetonide-terminated dendron derived from bis-MPA were synthesized *via* interchange of xanthates/reversible addition–fragmentation chain transfer polymerization (MADIX/RAFT) of NVP and "chain-first" strategy (Scheme 2). The successful synthesis of the desired LDBCs was confirmed by ^{1}H NMR spectra and GPC. The ^{1}HNMR spectra of PNVP-Phe-Lys-*b*-G_n (Fig. 1a, S1 and S2, ESI†) displayed characteristic signals attributed to linear PNVP chain (peaks d, e, f, g and h at 1.51–1.88 ppm, 3.49–4.09 ppm, 2.95–3.47 ppm, 1.88–2.14 ppm and 2.14–2.63 ppm, respectively) and acetonide-terminated bis-MPA dendrons (peaks b′, a′ and c′ at 3.49–4.09 ppm, 1.43 ppm, respectively). All copolymers showed unimodal symmetrical GPC curves (Fig. 2) with narrow molecular weight distributions (PDI ≤ 1.25, Table 1) and their $M_{n,GPC}$ increase with increased generation of the dendron which indicated the synthesis of three generations of LDBCs.

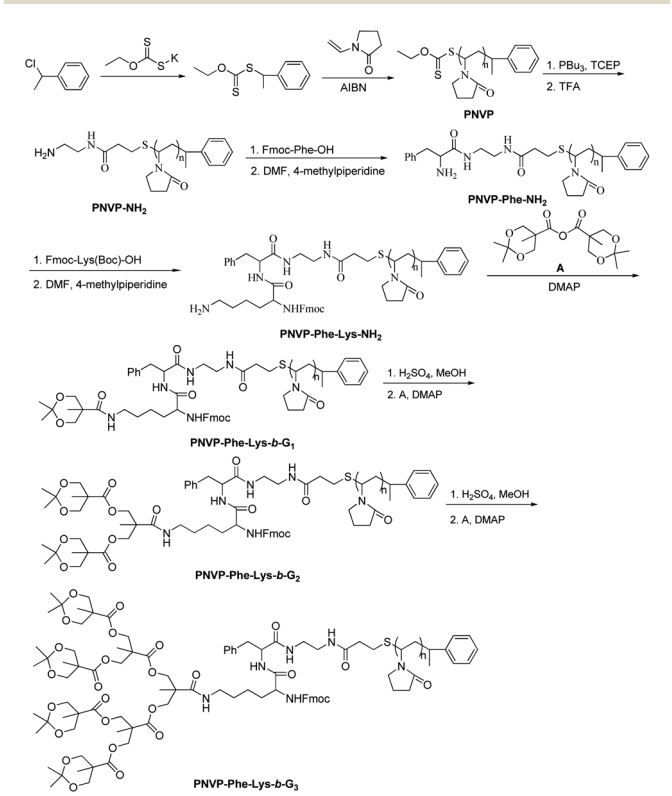

Scheme 2 Synthesis of PNVP-Phe-Lys-*b*-G_n (n = 1–3).

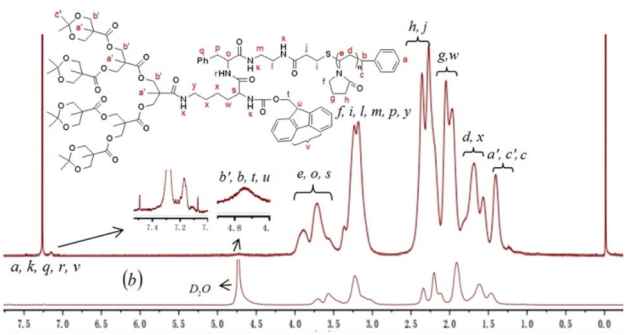

Fig. 1 ^{1}H NMR spectra of PNVP-Phe-Lys-*b*-G_3 in $CDCl_3$ (a) and D_2O (b).

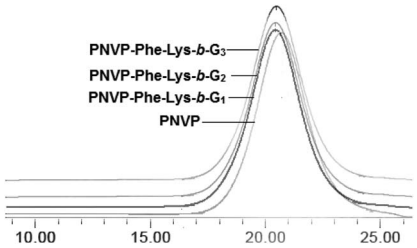

Fig. 2 GPC traces of PNVP-Phe-Lys-*b*-G_n (n = 1–3).

Self-assembly behavior

PNVP-Phe-Lys-*b*-G_n (n = 1–3) are amphiphilic and can therefore self-assemble into micelles in aqueous media. The fluorescence probe technique, ^{1}H NMR spectra, transmission electron microscopy (TEM) and particle size analysis were used to examine the self-organization of the amphiphilic LDBCs in water. The critical micelle concentration (CMC) values of PNVP-Phe-Lys-*b*-G_n (n = 1–3) was evaluated by fluorescence techniques using pyrene as a probe. As shown in Fig. 3, they are 0.056, 0.0316, 0.0158 mg mL^{-1}, respectively, which decrease with the increase of the acetonide-terminated bis-MPA dendrons, indicating that the copolymer is more likely to form stable micelles as the generation of the LDBCs increases.[43,44] The self-assembly behavior of the copolymers was further investigated by ^{1}H NMR spectroscopy. When the ^{1}H NMR experiments of the PNVP-Phe-Lys-*b*-G_3 were performed in D_2O, the methyl proton peaks of at the end of the acetonide-terminated bis-MPA dendrons were highly suppressed (Fig. 1b), indicating the formation of core–shell micellar structure in the aqueous environment, thereby restricting the motion of methyl protons within the hydrophobic core.[45,46] Average hydrodynamic diameters of PNVP-Phe-Lys-*b*-G_n (n = 1–3) micelles determined by particle sizing measurements ranged from 110 nm to 270 nm (Fig. 4), which increases with increasing the generation of the LDBCs. TEM images showed that PNVP-Phe-Lys-*b*-G_3 was able to self-assemble into spherical micelles (Fig. 5a).

Enzymatic responsive properties

Trypsin can catalyze the hydrolysis of proteins and has a high degree of specificity for the bond between the carboxyl group of

Table 1 Characterizations of PNVP-Phe-Lys-*b*-G_n (n = 1–3)

Sample	$M_{n,th}$ (kDa)	$M_{n,GPC}$[c] (kDa)	$Đ^c = M_w/M_n$	Conversion (%)
PNVP	11.9[a]	21.2	1.24	77
PNVP-Phe-Lys-*b*-G_1	12.7[b]	21.4	1.25	—
PNVP-Phe-Lys-*b*-G_2	13.0[b]	21.6	1.24	—
PNVP-Phe-Lys-*b*-G_3	13.5[b]	21.8	1.24	—

[a] The theoretic molecular weight was calculated by the formula: $M_{n,th} = M_{monomer} \times$ ([monomer]/[initiator]) $\times$ conversion% + $M_{initiator}$. [b] The theoretic molecular weight was calculated by the formula: $M_{n,th}$ = $M_{n,th}$ of PNVP + M_{th} of Phe–Lys and G_n (n = 1–3). [c] M_n and $Đ$ were determined by GPC.

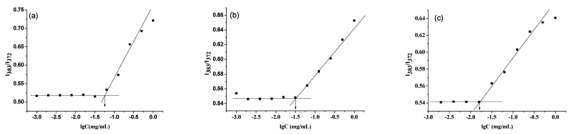

Fig. 3 Plots of I_{383}/I_{372} of pyrene emission spectra *versus* logarithm of concentration for PNVP-Phe-Lys-*b*-G_1 (a), PNVP-Phe-Lys-*b*-G_2 (b), PNVP-Phe-Lys-*b*-G_3 (c).

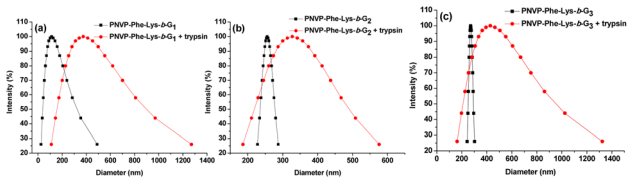

Fig. 4 The particle size of PNVP-Phe-Lys-*b*-G_1 (a), PNVP-Phe-Lys-*b*-G_2 (b), PNVP-Phe-Lys-*b*-G_3 (c) micelles and after the incubation with trypsin (75 μM).

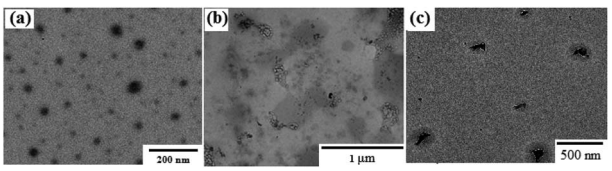

Fig. 5 TEM images of the formed micelles by PNVP-Phe-Lys-*b*-G_3 before (a) and after (b) the enzyme treatment at pH 7.4, at pH 5.0 (c).

basic amino acids (arginine, lysine) and other amino groups. Its high specificity is expressed as the choice of one end of the basic amino acid.[47–50] An enzymatically cleavable Phe–Lys dipeptide was incorporated between a hydrophobic dendron derived from bis-MPA and hydrophilic PNVP of the amphiphilic LDBCs (PNVP-Phe-Lys-*b*-G_n, n = 1–3). This dipeptide is a substrate for trypsin that is known to be overexpressed in pathological conditions such as cancer and inflammation.[39,51] Enzymatic cleavage at the Phe–Lys dipeptide will trigger disassembly of the LDBC micelles. To gain an insight into enzyme responsive disassembly of the micelles, PNVP-Phe-Lys-*b*-G_3 micelle solution was incubated with trypsin solution (75 μM) at 37 °C for 48 h. We observed that a large amount of white flocculation appeared (Fig. S3, ESI†), indicating that the Phe–Lys dipeptide between hydrophilic PNVP and a hydrophobic dendron derived from bis-MPA was disrupted by trypsin to trigger disintegration of the LDBC micelles, thus resulting in precipitation of the hydrophobic portion from solution to produce some white flocculation.

Nile red dye as a model payload was further employed to investigate enzyme responsive disassembly behavior of PNVP-Phe-Lys-*b*-G_n (n = 1–3) micelles. The fluorescence intensity of Nile red for all three generation of LDBCs showed no significant change in the absence of trypsin (Fig. 6), indicating that Nile red loaded micelles are stable. However, upon the addition of solutions of trypsin (25 μM or 75 μM) for 48 h, we observed that the purple-red dye-loaded micellar solutions of the LDBCs gradually became lighter in color and generated precipitates (Fig. S4, ESI†). In addition, the color of the micellar solution became lighter with increasing enzyme concentration. After 25 μM solution of trypsin was added, all three generation of LDBCs showed that the fluorescence intensity of Nile red decreased (Fig. 6), indicating that trypsin cleaves the peptide bond, which causes the copolymer to decompose into a hydrophilic part and hydrophobic part, and the micelles disassemble. The hydrophobic Nile red contained in the micelles is released, and the environment in which it is changed causes the fluorescence intensity to decrease, and the phenomenon becomes more pronounced with the increase of time. At the same enzyme concentration, the micelle solution color becomes lighter as the polymer generation increases and the disassembly rates of micelles decrease upon increase of the LDBCs generation, because the micelles becomes more stable with increasing hydrophobic peripheral ketal groups of the LDBCs, and trypsin is less accessible to the Phe–Lys dipeptide in the tightly packed higher generation dendrons. Similar phenomena were also observed in other amphiphilic dendrimer systems.[52] At the high enzyme concentration of 75 μM, the fluorescence intensity of

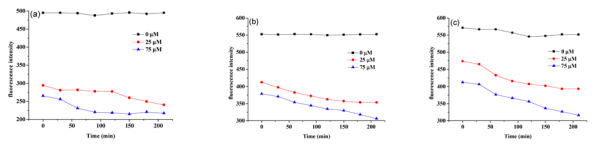

Fig. 6 Comparison of the disassembly rates (fluorescence assay) of micelles formed by PNVP-Phe-Lys-*b*-G_1 (a), PNVP-Phe-Lys-*b*-G_2 (b) and PNVP-Phe-Lys-*b*-G_3 (c) after the incubation with different concentrations of trypsin (0 μM, 25 μM and 75 μM).

Nile red was similar to that of trypsin at 25 μM, except that the disassembly rate of micelles was faster as the concentration of trypsin increased. The size change of the LDBC micelles in response to trypsin hydrolysis was followed by particle sizing measurement. As shown in Fig. 4, the particle size of the micelles increased significantly after the addition of trypsin. When the different concentrations of trypsin were added, the particle size of the micelles increased with the increase of the enzyme concentration (Fig. S5, ESI†). This is because high concentrations of trypsin have a greater probability of contact with the micelles to lead to disassembly of the micelles. The enzyme triggered disassembly of the LDBC micelles was confirmed by TEM measurement. As shown in Fig. 5b, small pieces and large aggregates instead of spherical micelles in the presence of trypsin were observed in the TEM images, further confirming enzymatic responsive degradation of the copolymers.

pH–responsive properties

The pH–responsive disassembly of LDBC micelles was first investigated by monitoring the change in the fluorescence of encapsulated Nile red dyes at pH 5.0 (tumor acidic environment[53,54]) and pH 7.4 (blood environment[55]). As plotted in Fig. 7, S6 and S7 (ESI†), no obvious change in the fluorescence intensities was observed throughout 48 h at pH 7.4, indicating that the micelles were stable under neutral conditions. But time dependent decreases in fluorescence intensity of Nile red were observed for all three generation of LDBCs at pH 5.0 (Fig. 8). The spherical nanostructures could no longer be found for PNVP-Phe-Lys-*b*-G_3 in the TEM image of buffer solution at pH 5.0 (Fig. 5c), further confirming pH responsive degradation of the LDBCs. This could be attributed to the fact that the hydrophobic dendritic end groups of the LDBCs are composed of acid-sensitive ketal groups, which can be cleaved under mildly acidic conditions. Upon cleavage of the ketal groups, the LDBCs were converted from amphiphilic to hydrophilic, thereby destroying the assembly of micelles, triggering the release of Nile red and the decrease of fluorescence intensity. Furthermore, we observed that disassembly rates of the LDBC micelles decreased with increase in the generation of bis-MPA dendrons at pH 5.0. This effect of the generation on the disassembly rate is similar to that observed in enzyme triggered disintegration of the LDBC micelles,[9] which is probably because the protons in buffer solution could not penetrate into the hydrophobic core of the micelle and instead the hydrolysis of peripheral ketal groups occur at the non-assembled LDBC molecules in the solution, which are in equilibrium with the micellar assemblies.

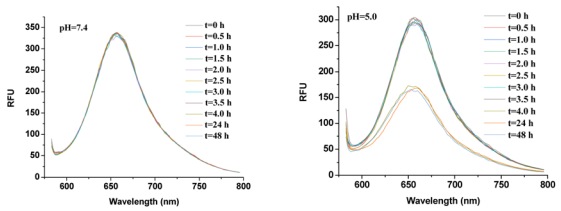

Fig. 7 Fluorescence spectra of Nile red in PNVP-Phe-Lys-*b*-G_3 micelles at pH 7.4 and pH 5.0.

Enzyme and pH dual responsive properties

To study enzyme and pH dual responsive disassembly behavior of the LDBCs micelles, the Nile red loaded LDBC solution was subjected to trypsin (75 μM) and acetate buffer of pH 5.0 and fluorescence intensity was monitored with the progress of time. The decrease in fluorescence intensity upon the addition of trypsin at pH 5.0 was much faster than either in the presence of enzyme or buffer solution of pH 5.0 over the same time period (Fig. 9), which corroborates the fact that disassembly rate of the micelles at pH 5.0 can be accelerated by adding trypsin solution. The reason was that simultaneous cleavage of the dipeptide Phe–Lys linkage as well as the peripheral ketal groups of the LDBCs in the presence of pH and enzyme dual stimuli caused a rapid disassembly of the micelles, thus providing an enhancement in the release kinetics of the loaded Nile red.

In vitro drug release from PTX-loaded micelles

Paclitaxel (PTX) was used as a model drug to assess the suitability of PNVP-Phe-Lys-*b*-G_3 micelles as anti-cancer drug delivery carriers. The drug loading content and encapsulation efficiency were determined by a UV spectrometer. The results exhibited that PTX was successfully incorporated into LDBC

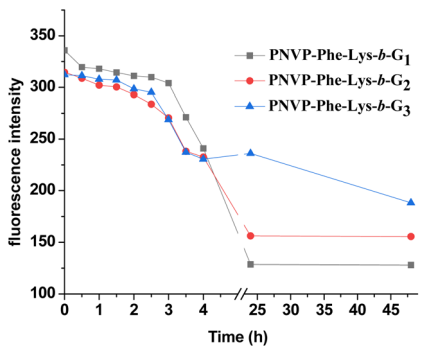

Fig. 8 Comparison of the disassembly rates (fluorescence assay) of micelles formed by PNVP-Phe-Lys-*b*-G_1, PNVP-Phe-Lys-*b*-G_2 and PNVP-Phe-Lys-*b*-G_3 at pH 5.0.

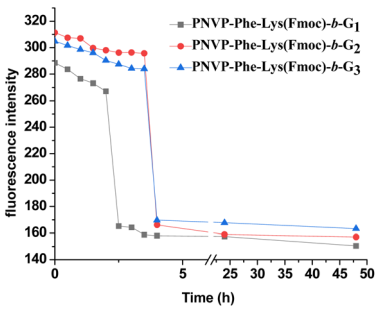

Fig. 9 Comparison of the disassembly rates (fluorescence assay) of micelles formed by PNVP-Phe-Lys-*b*-G_1, PNVP-Phe-Lys-*b*-G_2 and PNVP-Phe-Lys-*b*-G_3 after the incubation with trypsin (75 μM) at pH 5.0.

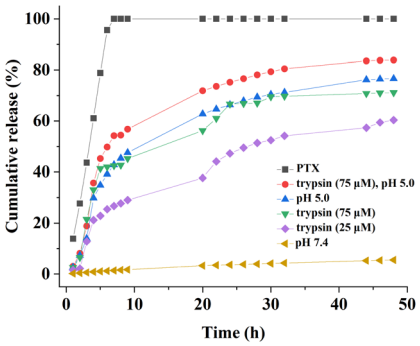

Fig. 10 *In vitro* PTX release profiles of the PTX-loaded PNVP-Phe-Lys-*b*-G_3 micelles at 37 °C under different stimuli conditions.

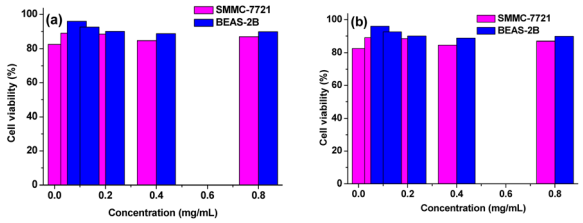

Fig. 11 Cell viability of BEAS-2B and SMMC-7721 cells following 48 h of incubation with PNVP-Phe-Lys-*b*-G_2 (a) and PNVP-Phe-Lys-*b*-G_3 (b) micelles.

micelles, and the entrapment efficiency (EE) and drug loading content (DLC) were 81.36% and 5.5%, respectively. In comparison with the blank micelles, the size of the PTX-loaded micelles increased to 381 nm (Fig. S8, ESI†). These PTX-loaded LDBC micelles have been found to be very stable, showing no significant changes in average particle size over 30 days (Fig. S8, ESI†). The release of PTX from PNVP-Phe-Lys-*b*-G_3 micelles was investigated in buffer solution (pH 7.4 or pH 5.0) and in presence or absence of 25 μM or 75 μM trypsin at 37 °C (Fig. 10). It could be observed that the release rates of PTX from the micelles were markedly influenced by trypsin. In presence of 25 μM or 75 μM trypsin, the drug loaded micelles showed a much faster drug release rate and 28–42% of the loaded PTX was released within 10 h, while only a small amount of PTX are released within 48 h in absence of trypsin at pH 7.4. Compared with the release at this relatively low trypsin concentration (25 μM), PTX-release from micelles at the high trypsin concentration of 75 μM is much faster. The rate and amount of drug release was found to be much faster at pH 5.0 than that at pH 7.4, exhibiting a stronger dependence of the release rate on pH values. Interestingly, the release rate of PTX from the LDBC micelles in buffer solution at pH 5.0 is faster than those upon the addition of the activating enzyme. This could be attributed to the fact that the protons in buffer solution are more accessible to peripheral ketal groups of the LDBCs while the enzymatic substrate Phe–Lys dipeptide is at the junction point between linear chain and dendritic block of LDBCs, which is less accessible to the enzyme. This result further supported the equilibrium-based activation mechanism, which was described previously for enzyme responsive assemblies[9,55] and above mentioned for pH responsive assemblies. More importantly, the fastest PTX release rate was observed in both pH and enzyme stimuli and the accumulative PTX release (83% of PTX released after 48 h) was higher than that in a single stimulus, suggesting that combination of two stimuli could significantly accelerate and more complete release of the loaded drug.

In vitro cytotoxicity study

Cytotoxic effects of PNVP-Phe-Lys-*b*-G_2 and PNVP-Phe-Lys-*b*-G_3 were investigated using the MTS assay against cultured human lung epithelial cells (BEAS-2B) and human liver cancer cells (SMMC-7721). As shown in Fig. 11, the LDBCs exhibited more than 85% cell viability over a concentration range of 0.05–800 μg mL^{-1} regardless of cell type after 48 h of culture. In addition, cell viability was not significantly influenced by the concentration of the LDBCs. These results showed that LDBCs have a good biocompatibility within limit concentration and were suitable for drug delivery.

Conclusions

In summary, a dipeptide Phe–Lys linkage was introduced, as an artificial enzyme active site, at amphiphilic linear-dendritic block copolymers (LDBCs) junction and the LDBCs were decorated with peripheral ketal groups, which endowed their enzyme and pH dual responsiveness. Three generations of well-defined amphiphilic LDBCs, PNVP-Phe-Lys-*b*-G_n (n = 1–3) were synthesized by a combination of MADIX/RAFT polymerization and "chain-first" strategy. They could self-assemble into spherical nanomicelles and disassembly to release loaded drug in various microenvironment which typically exist in cancer cells. In particular, release of the loaded drug could be tuned by changing the generation of the LDBCs. Additionally, the results of cell viability assays indicated that the LDBCs were nontoxic up to a tested concentration (800 μg mL^{-1}). This study not only enriches the structure types of LDBCs, but also provides novel drug carriers for smart drug delivery systems.

Author contributions

Y. Wang and W. Song: synthesis, investigation, writing-original draft. L. Bao: investigation. J. Wei and Y. Qian: investigation. Y. Bi: conceptualization, supervision, methodology, writing-review & editing, funding acquisition.

Conflicts of interest

There are no conflicts to declare.

Acknowledgements

The authors gratefully acknowledge the support for this study from the National Natural Science Foundation of China (21564017).

Notes and references

1 E. Blasco, M. Piñol and L. Oriol, Responsive linear-dendritic block copolymers, *Macromol. Rapid Commun.*, 2014, **35**, 1090–1115.
2 G. Liu, W. Liu and C. M. Dong, UV- and NIR-responsive polymeric nanomedicines for on-demand drug delivery, *Polym. Chem.*, 2013, **4**, 3431–3443.
3 X. Liu, F. M. Yavitt and I. Gitsov, Supramolecular linear-dendritic nanoreactors: Synthesis and catalytic activity in "green" Suzuki-Miyaura reactions, *Polymers*, 2023, **15**, 1671.
4 L. Zhu, G. Zhu, M. Li, E. Wang, R. Zhu and X. Qi, Thermosensitive aggregates self-assembled by an asymmetric block copolymer of dendritic polyether and poly(*N*-isopropylacrylamide), *Eur. Polym. J.*, 2002, **38**, 2503–2506.
5 E. R. Gillies, T. B. Jonsson and J. M. J. Fréchet, Stimuli-responsive supramolecular assemblies of linear-dendritic copolymers, *J. Am. Chem. Soc.*, 2004, **126**, 11936–11943.
6 V. Percec, D. Sahoo and J. Adamson, Stimuli-responsive principles of supramolecular organizations emerging from self-assembling and self-organizable dendrons, dendrimers, and dendronized polymers, *Polymers*, 2023, **15**, 1832.
7 S. Han, P. Xin, Q. Guo, Z. Cao, H. Huang and J. Wu, Oral delivery of protein drugs *via* lysine polymer-based nanoparticle platforms, *Adv. Healthcare Mater.*, 2023, 2300311.
8 X. You, L. Wang, L. Wang and J. Wu, Rebirth of aspirin synthesis by-product: prickly poly (salicylic acid) nanoparticles as self-anticancer drug carrier, *Adv. Funct. Mater.*, 2021, **31**, 2100805.
9 A. J. Harnoy, I. Rosenbaum, E. Tirosh, Y. Ebenstein, R. Shaharabani, R. Beck and R. J. Amir, Enzyme-responsive amphiphilic PEG-dendron hybrids and their assembly into smart micellar nanocarriers, *J. Am. Chem. Soc.*, 2014, **136**, 7531–7534.
10 J. Hu, G. Zhang and S. Liu, Enzyme-responsive polymeric assemblies, nanoparticles and hydrogels, *Chem. Soc. Rev.*, 2012, **41**, 5933–5949.
11 T. Kuang, Y. Liu, T. Gong, X. Peng, X. Hu and Z. Yu, Enzyme-responsive nanoparticles for anticancer drug delivery, *Curr. Nanosci.*, 2016, **12**, 38–46.
12 Y. Ding, Y. Kang and X. Zhang, Enzyme-responsive polymer assemblies constructed through covalent synthesis and supramolecular strategy, *Chem. Commun.*, 2015, **51**, 996–1003.
13 M. Zelzer, S. J. Todd, A. R. Hirst, T. O. McDonald and R. V. Ulijn, Enzyme responsive materials: design strategies and future developments, *Biomater. Sci.*, 2013, **1**, 11–39.
14 M. Segal, R. Avinery, M. Buzhor, R. Shaharabani, A. J. Harnoy, E. Tirosh, R. Beck and R. J. Amir, Molecular precision and enzymatic degradation: from readily to undegradable polymeric micelles by minor structural changes, *J. Am. Chem. Soc.*, 2017, **139**, 803–810.
15 A. J. Harnoy, M. Buzhor, E. Tirosh, R. Shaharabani, R. Beck and R. J. Amir, Modular synthetic approach for adjusting the disassembly rates of enzyme-responsive polymeric micelles, *Biomacromolecules*, 2017, **18**, 1218–1228.
16 Y. Qian, D. You, F. Lin, J. Wei, Y. Wang and Y. Bi, Enzyme triggered disassembly of amphiphilic linear-dendritic block copolymer micelles based on poly[*N*-(2-hydroxyethyl-l-glutamine)], *Polym. Chem.*, 2019, **10**, 94–105.
17 J. Wei, F. Lin, D. You, Y. Qian, Y. Wang and Y. Bi, Self-assembly and enzyme responsiveness of amphiphilic linear-dendritic block copolymers based on poly(*N*-vinylpyrrolidone) and dendritic phenylalanyl–lysine dipeptides, *Polymers*, 2019, **11**, 1625.
18 E. R. Gillies and J. M. J. Fréchet, pH-responsive copolymer assemblies for controlled release of doxorubicin, *Bioconjugate Chem.*, 2005, **16**, 361–368.
19 L. Tian and P. T. Hammond, Comb-dendritic block copolymers as tree-shaped macromolecular amphiphiles for nanoparticle self-assembly, *Chem. Mater.*, 2006, **18**, 3976–3984.
20 J. C. M. van Hest, M. W. P. L. Baars, C. Elissen-Román, M. H. P. van Genderen and E. W. Meijer, Acid-functionalized amphiphiles, derived from polystyrene-poly (propylene imine) dendrimers, with a pH-dependent aggregation, *Macromolecules*, 1995, **28**, 6689–6691.
21 S. Khoee and K. Hemati, Synthesis of magnetite/polyamino-ester dendrimer based on PCL/PEG amphiphilic copolymers *via* convergent approach for targeted diagnosis and therapy, *Polymer*, 2013, **54**, 5574–5585.
22 L. Chen, T. Chen, W. Fang, Y. Wen, S. Lin, J. Lin and C. Cai, Synthesis and pH-responsive "schizophrenic" aggregation of a linear-dendron-like polyampholyte based on oppositely charged polypeptides, *Biomacromolecules*, 2013, **14**, 4320–4330.
23 D. Huang, Y. Wang, F. Yang, H. Shen, Z. Weng and D. Wu, Charge-reversible and pH-responsive biodegradable micelles and vesicles from linear-dendritic supramolecular amphiphiles for anticancer drug delivery, *Polym. Chem.*, 2017, **8**, 6675–6687.
24 H. E. Rogers, P. Chambon, S. E. Auty, F. Y. Hern, A. Owen and S. P. Rannard, Synthesis, nanoprecipitation and pH sensitivity of amphiphilic linear–dendritic hybrid polymers and hyperbranched-polydendrons containing tertiary amine functional dendrons, *Soft Matter*, 2015, **11**, 7005–7015.
25 H. Cai, P. Tan, X. Chen, M. Kopytynski, D. Pan, X. Zheng, L. Gu, Q. Gong, X. Tian, Z. Gu, H. Zhang, R. Chen and K. Luo, Stimuli-sensitive linear-dendritic block copolymer-drug prodrug as a nanoplatform for tumor combination therapy, *Adv. Mater.*, 2022, **34**, 2108049.
26 M. J. Heffernan and N. Murthy, Polyketal nanoparticles: a new pH-sensitive biodegradable drug delivery vehicle, *Bioconjugate Chem.*, 2005, **16**, 1340–1342.
27 D. Chen and H. Wang, Novel pH-sensitive biodegradable polymeric drug delivery systems based on ketal polymers, *J. Nanosci. Nanotechnol.*, 2014, **14**, 983–989.

28 Y. Qian, J. Wei, Y. Wang, D. You, F. Lin, W. Yue and Y. Bi, Thermal and enzymatic dual-stimuli responsive linear-dendritic block copolymers based on poly(*N*-vinylcaprolactam), *Polym. Adv. Technol.*, 2020, **31**, 2797–2805.
29 W. Song, J. Wei, L. Li, Y. Qian, Y. Wang and Y. Bi, Cathepsin B and thermal dual-stimuli responsive linear-dendritic block copolymer micelles for anticancer drug delivery, *Polym. Int.*, 2022, **71**, 317–327.
30 P. Schattling, F. D. Jochum and P. Theato, Multi-stimuli responsive polymers-the all-in-one talents, *Polym. Chem.*, 2014, **5**, 25–36.
31 Z. Q. Cao and G. J. Wang, Multi-stimuli-responsive polymer materials: Particles, films, and bulk gels, *Chem. Rec.*, 2016, **16**, 1398–1435.
32 X. Fu, L. Hosta-Rigau, R. Chandrawati and J. Cui, Multi-stimuli-responsive polymer particles, films, and hydrogels for drug delivery, *Chem*, 2018, **4**, 2084–2107.
33 J. L. Wike-Hooley, J. Haveman and H. S. Reinhold, The relevance of tumour pH to the treatment of malignant disease, *Radiother. Oncol.*, 1984, **2**, 343–366.
34 L. E. Gerweck and K. Seetharaman, Cellular pH gradient in tumor *versus* normal tissue: potential exploitation for the treatment of cancer, *Cancer Res.*, 1996, **56**, 1194–1198.
35 M. Kanamala, W. R. Wilson, M. Yang, B. D. Palmer and Z. Wu, Mechanisms and biomaterials in pH-responsive tumour targeted drug delivery: a review, *Biomaterials*, 2016, **85**, 152–167.
36 K. Kessenbrock, V. Plaks and Z. Werb, Matrix metalloproteinases: regulators of the tumor microenvironment, *Cell*, 2010, **141**, 52–67.
37 S. Ferber, H. Baabur-Cohen, R. Blau, Y. Epshtein, E. Kisin-Finfer, O. Redy, D. Shabat and R. Satchi-Fainar, Polymeric nanotheranostics for real-time non-invasive optical imaging of breast cancer progression and drug release, *Cancer Lett.*, 2014, **352**, 81–89.
38 J. Zhang, J. Gao, M. Chen and Z. Yang, Using phosphatases to generate self-assembled nanostructures and their applications, *Antioxid. Redox Signaling*, 2014, **20**, 2179–2190.
39 K. Soreide, E. A. Janssen, H. Körner and J. P. A. Baak, Trypsin in colorectal cancer: molecular biological mechanisms of proliferation, invasion, and metastasis, *J. Pathol.*, 2006, **209**, 147–156.
40 E. R. Gillies and J. M. J Fréchet, Designing macromolecules for therapeutic applications: polyester dendrimers poly(ethylene oxide) "bow-tie" hybrids with tunable molecular weight and architecture, *J. Am. Chem. Soc.*, 2002, **124**, 14137–14146.
41 M. Malkoch, E. Malmström and A. Hult, Rapid and efficient synthesis of aliphatic ester dendrons and dendrimers, *Macromolecules*, 2002, **35**, 8307–8314.
42 G. Tang, M. Hu, Y. Ma, D. You and Y. Bi, Synthesis and solution properties of novel thermo-and pH-responsive poly(*N*-vinylcaprolactam)-based linea-dendritic block copolymers, *RSC Adv.*, 2016, **6**, 42786–42793.
43 J. C. M. van Hest, D. A. P. Delnoye, M. W. P. L. Baars, M. H. P. van Genderen and E. W. Meijer, Polystyrene-dendrimer amphiphilic block copolymers with a generation-dependent aggregation, *Science*, 1995, **268**, 1592–1595.
44 X. Liu and I. Gitsov, Nonionic amphiphilic linear dendritic copolymers. Morphology tuning by solvent-induced self-assembly, *Macromolecules*, 2019, **52**, 5563–5573.
45 Y. Li, K. Xiao, J. Luo, J. Lee, S. Pan and K. S. Lam, A novel size-tunable nanocarrier system for targeted anticancer drug delivery, *J. Controlled Release*, 2010, **144**, 314–323.
46 Y. Li, K. Xiao, J. Luo, W. Xiao, J. S. Lee, A. M. Gonik, J. Kato, T. A. Dong and K. S. Lam, Well-defined, reversible disulfide cross-linked micelles for on-demand paclitaxel delivery, *Biomaterials*, 2011, **32**, 6633–6645.
47 J. V. Olsen, S. E. Ong and M. Mann, Trypsin cleaves exclusively C-terminal to arginine and lysine residues, *Mol. Cell. Proteomics*, 2004, **3**, 608–614.
48 K. Rose, R. Stöcklin, L. A. Savoy, P. O. Regamey, R. E. Offord, P. Vuagnat and J. Markussen, Reaction mechanism of trypsin-catalysed semisynthesis of human insulin studied by fast atom bombardment mass spectrometry, *Protein Eng., Des. Sel.*, 1991, **4**, 409–412.
49 P. Chanphai and H. A. Tajmirriahi, Trypsin and trypsin inhibitor bind PAMAM nanoparticles: Effect of hydrophobicity on protein–polymer conjugation, *J. Colloid Interface Sci.*, 2016, **461**, 419–424.
50 R. Månsson, G. Frenning and M. Malmsten, Factors affecting enzymatic degradation of microgel-bound peptides, *Biomacromolecules*, 2013, **14**, 2317–2325.
51 G. Ma, W. Lin, Z. Yuan, J. Wu, H. Qian, L. Xu and S. Chen, Development of ionic strength/pH/enzyme triple-responsive zwitterionic hydrogel of the mixed L-glutamic acid and L-lysine polypeptide for site-specific drug delivery, *J. Mater. Chem. B*, 2017, **5**, 935–943.
52 M. A. Azagarsamy, P. Sokkalingam and S. Thayumanavan, Enzyme-triggered disassembly of dendrimer-based amphiphilic nanocontainers, *J. Am. Chem. Soc.*, 2009, **131**, 14184–14185.
53 H. Wei, R. X. Zhuo and X. Z. Zhang, Design and development of polymeric micelles with cleavable links for intracellular drug delivery, *Prog. Polym. Sci.*, 2013, **38**, 503–535.
54 C. I. C. Crucho, Stimuli-responsive polymeric nanoparticles for nanomedicine, *ChemMedChem*, 2015, **10**, 24–38.
55 A. J. Harnoy, G. Slor, E. Tirosh and R. J. Amir, The effect of photoisomerization on the enzymatic hydrolysis of polymeric micelles bearing photo-responsive azobenzene groups at their cores, *Org. Biomol. Chem.*, 2016, **14**, 5813–5819.